Iterative Sound Speed Tomography for Distributed Aberration Correction

Rehman Ali*, Trevor Mitcham*, Melanie Singh†, Richard Bouchard‡,
Marvin Doyley§, Jeremy Dahl¶, Nebojsa Duric*†§
Department of Imaging Sciences, University of Rochester Medical Center, Rochester, NY, USA *
Department of Biomedical Engineering, University of Rochester, Rochester, NY, USA †
Department of Imaging Physics, University of Texas MD Anderson Cancer Center, Houston, TX, USA‡
Department of Electrical Engineering, University of Rochester, Rochester, NY, USA §
Department of Radiology, Stanford University, Stanford, CA, USA ¶
Email: Rehman_Ali@URMC.Rochester.edu, Trevor_Mitcham@URMC.Rochester.edu,
melaniesingh@rochester.edu, RRBouchard@mdanderson.org, m.doyley@rochester.edu,
jjdahl@stanford.edu, Nebojsa_Duric@URMC.Rochester.edu

2023 IEEE International Ultrasonics Symposium (IUS) | 979-8-3503-4645-9/23/$31.00 ©2023 IEEE | DOI: 10.1109/IUS51837.2023.10306695

***Abstract*—In pulse-echo ultrasound imaging, there exists a strong duality between sound speed estimation and aberration correction. This has led to the development of closed-loop iterative frameworks that address both estimation and correction simultaneously. This work revisits previous work on wave-equation migration velocity analysis (WEMVA) to derive and explain our new closed-loop solution to the problem based on a waveform inversion-style approach: full-waveform iterative model-based phase aberration computed tomography (Full-Waveform IMPACT). Full-Waveform IMPACT reproduces the same velocity-depth ambiguities that many previous works have described. However, by approaching the problem using a waveform inversion-style method, we demonstrate that the velocity-depth ambiguity is intricately tied to the problem of cycle skipping and false local minima.**

***Index Terms*—Medical Pulse-Echo Ultrasound Imaging, Adjoint-State Method, Wave-Equation Migration Velocity Analysis, Full Waveform Inversion**

I. Introduction

Although spatial variations in sound speed were always understood to be the cause of phase aberration in medical pulse-echo ultrasound imaging, the modeling and correction of aberration remained limited to phase screen models [1], [2] and time reversal [3] approaches until recent efforts to directly reconstruct the sound speed profile in tissue from phase aberrations [4]–[6].

These works motivated a new set of approaches to correct for aberrations in the image based on knowledge of the sound speed profile in the tissue [7], [8]. A major limitation identified in recent works [9] is that the average sound speed or depth-wise variation in sound speed falls in the null-space of the aberration delay measurement process. In other words, the reflection tomography described in prior works [4]–[6] would not be able to accurately recover a bulk error in sound speed. Instead, reflection tomography is more likely to estimate a near-field disturbance that compensates for a bulk error in sound speed. In the seismic imaging literature, this problem has been dubbed the velocity-depth ambiguity [10].

Our recent work [11], [12] exploits the duality between sound speed estimation and phase aberration correction to solve both problems using a closed-loop approach known as iterative model-based phase aberration computed tomography (IMPACT). While most of the prior literature uses a single set of observed aberration delays or phase shifts to reconstruct sound speed, we use an iterative procedure in which aberrations in the image are used to reconstruct the sound speed profile, which is in turn used to re-image the medium, estimate a new set of aberration delays, and update the sound speed profile in the medium. Despite this closed-loop approach, IMPACT reproduces the velocity-depth ambiguity. The IMPACT method has been made open source: https://github.com/rehmanali1994/IMPACT.

We have also previously investigated a seismic imaging technique known as wave-equation migration velocity analysis (WEMVA) [13], [14]. If fully implemented in pulse-echo ultrasound, WEMVA would offer a diffraction-based closed-loop solution to the estimation-correction problem. However, major memory and computational limitations restricted this prior work to a single point target example. In this work, we modify the formulation of WEMVA in [14] to consider a ray-based migration velocity analysis (MVA) that leverages the strengths of WEMVA while reducing computational cost.

II. Theory and Methods

A. Delay-and-Sum Beamforming Model

We first begin with a multistatic synthetic aperture dataset $\tilde{p}_{mn}(t)$ indexed by single-element transmit m and receiver n as a function of time t. For an N-element array, let τ_{lk} refer to the time delay from element l to an image point $\vec{x}_k^{im}$. As per Figure 1, we can focus the full matrix of transmit and receive signals at each image point $\vec{x}_k^{im}$ by applying focusing delays:

$$p_{mn}(\vec{x}_k^{im}; \vec{s}) = \tilde{p}_{mn}(\tau_{mk}(\vec{s}) + \tau_{nk}(\vec{s})) \tag{1}$$

The result can then be summed over the receivers to obtain complex-valued images for each single-element transmit:

$$I_m(\vec{x}_k^{im}; \vec{s}) = \sum_{n=1}^{N} p_{mn}(\vec{x}_k^{im}; \vec{s}). \tag{2}$$

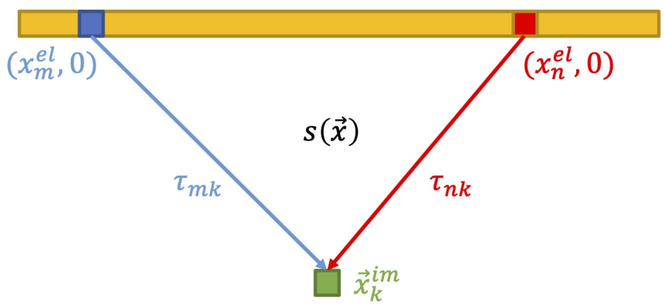

Fig. 1. Schematic for the time-of-flight of the ultrasound wave from transmitter m at $(x_m^{el}, 0)$ to image point $\vec{x}_k^{im}$ back to receiver n at $(x_n^{el}, 0)$. The time of flight is the line integral of slowness over the path

The objective function for the least-squares formulation of WEMVA [13], [14] would be

$$J(\vec{s}) = \frac{1}{2} \sum_{k} \sum_{m=1}^{N-1} \left| R_m(\vec{x}_k^{im}; \vec{s}) \right|^2, \tag{3}$$

where $R_m(\vec{x}_k^{im}; \vec{s}) = I_{m+1}(\vec{x}_k^{im}; \vec{s}) - I_m(\vec{x}_k^{im}; \vec{s})$ are the differences between images from adjacent transmitters.

B. Gradient with Respect to Slowness

The gradient of the objective function with respect to slowness is:

$$\frac{\partial J}{\partial \vec{s}} = Re \left\{ \sum_{k} \sum_{m=1}^{N-1} \left(\frac{\partial R_m(\vec{x}_k^{im})}{\partial \vec{s}} \right)^H R_m(\vec{x}_k^{im}) \right\}, \tag{4}$$

where $\frac{\partial R_m(\vec{x}_k^{im})}{\partial \vec{s}} = \frac{\partial I_{m+1}(\vec{x}_k^{im})}{\partial \vec{s}} - \frac{\partial I_m(\vec{x}_k^{im})}{\partial \vec{s}}$, and $(\cdot)^H$ is the Hermitian (or conjugate) transpose.

However, this also requires a way to compute $\frac{\partial I_m(\vec{x}_k^{im})}{\partial \vec{s}}$. As in past work [8], the time-of-flight τ_{lk} would be defined as the line integral of slowness (vectorized as $\vec{s}$) over the path from element l to image point $\vec{x}_k^{im}$. Therefore, we take the gradient of the delay-and-sum process as follows:

$$\begin{aligned} \frac{\partial I_m(\vec{x}_k^{im})}{\partial \vec{s}} &= \sum_{n=1}^{N} \frac{\partial p_{mn}(\vec{x}_k^{im})}{\partial \vec{s}} \\ &= \sum_{n=1}^{N} \left[\frac{\partial p_{mn}}{\partial t} (\tau_{mk} + \tau_{nk}) \right] \left(\frac{\partial \tau_{mk}}{\partial \vec{s}} + \frac{\partial \tau_{nk}}{\partial \vec{s}} \right), \end{aligned} \tag{5}$$

where $\left[\frac{\partial p_{mn}}{\partial t} (\tau_{mk} + \tau_{nk}) \right]$ is the application of focusing delays to the time-derivative of the multistatic channel data, and $\frac{\partial \tau_{lk}}{\partial \vec{s}}$ is the matrix of path lengths over each pixel of the slowness map from element l to image point $\vec{x}_k^{im}$.

Note that $\frac{\partial \tau_{mk}}{\partial \vec{s}}$ and $\frac{\partial \tau_{nk}}{\partial \vec{s}}$ correspond to transmit and receive paths, respectively. The aberration delay model in IMPACT essentially says that each single-element transmit image involves the same receive paths back to the transducer; therefore, any aberration delays between images $I_m(\vec{x}_k^{im}; \vec{s})$ and $I_{m+1}(\vec{x}_k^{im}; \vec{s})$ should be due to the difference in the transmit paths back to the transducer because the receive paths should cancel. However, when computing $R_m(\vec{x}_k^{im}; \vec{s})$, the receive paths do not cancel. There are nonzero contributions of $\left[\frac{\partial p_{m+1,n}}{\partial t} (\tau_{m+1,k} + \tau_{nk}) - \frac{\partial p_{mn}}{\partial t} (\tau_{mk} + \tau_{nk}) \right]$ along the receive path lengths $\frac{\partial \tau_{nk}}{\partial \vec{s}}$. This demonstrates the engagement of both transmit and receive paths in the tomography problem defined by the objective function (3).

C. Grouping Terms by Ray Path

For $m = 1, ..., N-1$ and $n = 1, ..., N$, we define the following auxiliary variables $u_{mn}(\vec{x}_k^{im})$ and $v_{mn}(\vec{x}_k^{im})$:

$$u_{m+1,n}(\vec{x}_k^{im}) = \left[\frac{\partial p_{m+1,n}^*(\vec{x}_k^{im})}{\partial t} \right] R_m(\vec{x}_k^{im}; \vec{s}), \tag{6}$$

$$v_{mn}(\vec{x}_k^{im}) = \left[\frac{\partial p_{mn}^*(\vec{x}_k^{im})}{\partial t} \right] R_m(\vec{x}_k^{im}; \vec{s}), \tag{7}$$

where the $*$ in the superscripts refers to complex conjugation. We can then find the single value $b_l(\vec{x}_k^{im})$ to backproject along the path from each image point $\vec{x}_k^{im}$ to each element l:

$$b_l(\vec{x}_k^{im}) = \begin{cases} Re\Big\{ -\sum_{n=1}^{N} v_{1,n}(\vec{x}_k^{im}) + \\ \quad \sum_{m=2}^{N} u_{m,1}(\vec{x}_k^{im}) - \sum_{m=1}^{N-1} v_{m,1}(\vec{x}_k^{im}) \Big\}, & l = 1 \\ Re\Big\{ \sum_{n=1}^{N} u_{N,n}(\vec{x}_k^{im}) + \\ \quad \sum_{m=2}^{N} u_{m,N}(\vec{x}_k^{im}) - \sum_{m=1}^{N-1} v_{m,N}(\vec{x}_k^{im}) \Big\}, & l = N \\ Re\Big\{ \sum_{n=1}^{N} \left(u_{ln}(\vec{x}_k^{im}) - v_{ln}(\vec{x}_k^{im}) \right) + \\ \quad \sum_{m=2}^{N} u_{ml}(\vec{x}_k^{im}) - \sum_{m=1}^{N-1} v_{ml}(\vec{x}_k^{im}) \Big\}. & \text{otherwise} \end{cases} \tag{8}$$

The gradient in equation (4) can then be computed as

$$\frac{\partial J}{\partial \vec{s}} = Re \left\{ \sum_{k} \sum_{l=1}^{N} b_l(\vec{x}_k^{im}) \left(\frac{\partial \tau_{lk}}{\partial \vec{s}} \right)^T \right\}. \tag{9}$$

The form of equation (9) shows that the gradient of the objective function can be computed by backprojecting $b_l(\vec{x}_k^{im})$. Any adjoint-state method can be used to achieve this. This means that path-length matrices do not actually have to be computed or stored. Additionally, the computation of $b_l(\vec{x}_k^{im})$ is practically the same as in WEMVA [14], so rather than backprojecting along a ray, WEMVA would backproject $b_l(\vec{x}_k^{im})$ along "wave-paths" from the transducer to the image point.

The common mid-angle (CMA) concept [6] is another way to probe both transmit and receive paths to an image point. The Full-Waveform IMPACT framework could be applied to

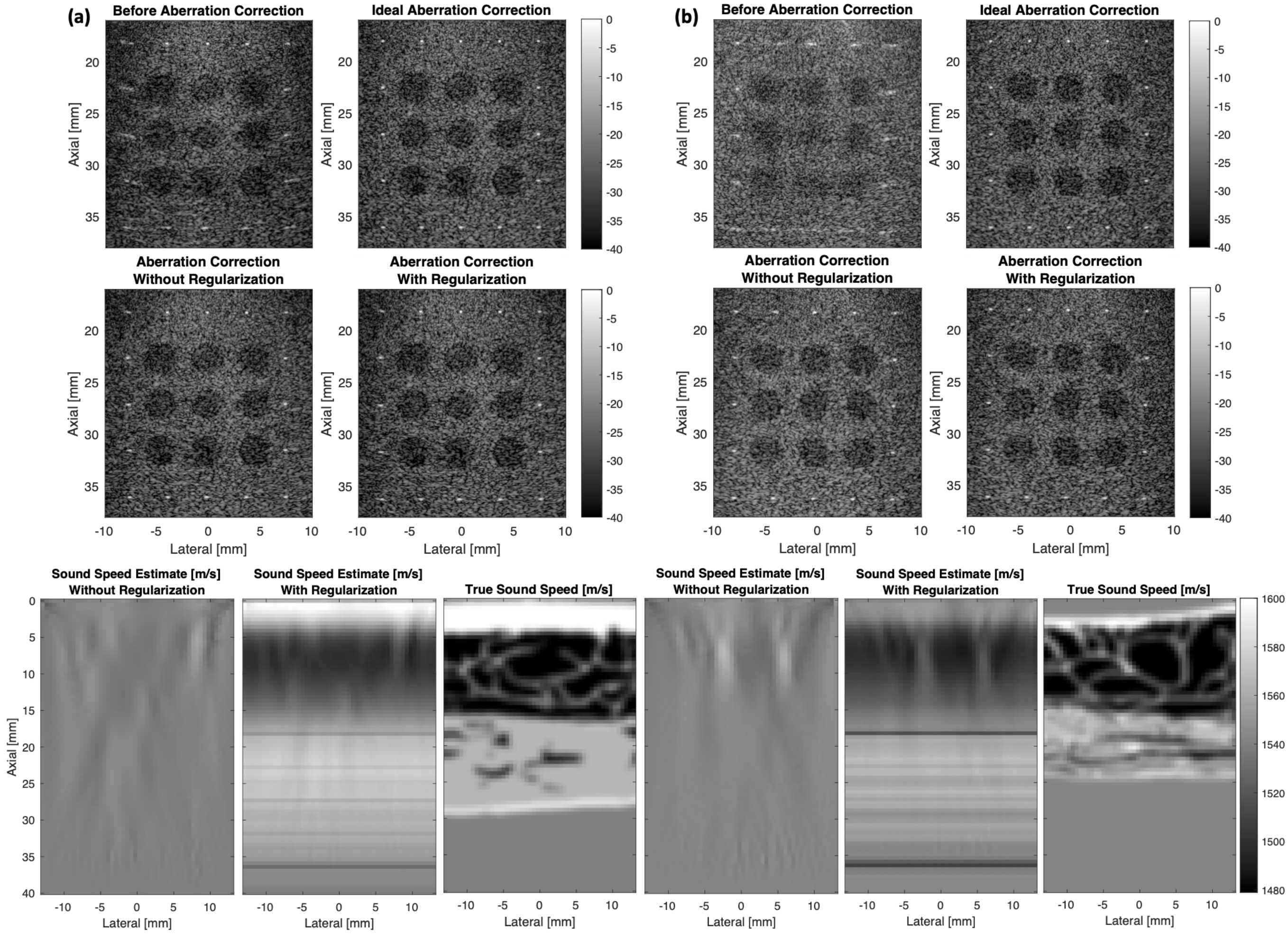

Fig. 2. Full-Waveform IMPACT in two different simulated abdominal imaging cases (a) and (b). In each case, we show the B-mode images before aberration correction, after the ideal correction using the true sound speed profile, and the full-waveform IMPACT corrections with ($\alpha = 0.999$) and without ($\alpha = 0.0$) layered medium regularization on the sound speed reconstruction. The corresponding sound speed reconstructions with and without regularization are shown alongside the true sound speed image in each case.

differences between images sharing a CMA, which would only modify the calculation of $b_l(\vec{x}_k^{im})$ in the backprojection formula (9).

D. Regularization

Similar to our past work on IMPACT [11], we include a layered medium regularization. However, here that layered medium regularization is achieved by modifying the gradient:

$$\left(\frac{\partial J}{\partial \vec{s}}\right)_{\text{used}} = \alpha \left(\frac{\partial J}{\partial \vec{s}}\right)_{\text{layer}} + (1-\alpha)\left(\frac{\partial J}{\partial \vec{s}}\right)_{\text{orig}}, \tag{10}$$

where $\left(\frac{\partial J}{\partial \vec{s}}\right)_{\text{orig}}$ refers to the original gradient calculation resulting from equation (9), $\left(\frac{\partial J}{\partial \vec{s}}\right)_{\text{layer}}$ is the result of layer-wise averaging the gradient values at each imaging depth, and $\left(\frac{\partial J}{\partial \vec{s}}\right)_{\text{used}}$ is the final gradient calculation used in the conjugate gradient algorithm described in the next section. We consider $\alpha = 0.0$ (no layered medium prior) and $\alpha = 0.999$ (strongly layered medium assumption).

E. Conjugate Gradient Algorithm

The same conjugate gradient algorithm described in the prior WEMVA work [14] is now being used in this ray-based approach, which we call full-waveform iterative model-based phase aberration computed tomography (Full-Waveform IMPACT). A total of 100 iterations of the conjugate gradient method are used. However, rather than keep the step size scaling parameter γ smaller than 1, we purposely increase its value to accelerate convergence in a manner that is dependent on the strength of the layered medium assumption α:

$$\gamma = 2\left(1 - \log(1-\alpha)\right). \tag{11}$$

F. Experimental Methods

The two k-Wave simulations [15] used in Figure 5 of [11] were used to test Full-Waveform IMPACT. These particular simulated datasets have already been made publicly available: https://github.com/rehmanali1994/IMPACT.

III. Results and Discussion

Figure 2 shows the result of Full-Waveform IMPACT in each of two different k-Wave simulations. Regularization has a significant impact on the axially-varying component of the sound speed reconstruction. Although, the resulting impact of this regularization on B-mode image quality is minor, the depth placement of imaging targets are significantly affected.

Without regularization ($\alpha = 0.0$), Full-Waveform IMPACT does not change the depth placement of image targets. On the other hand, a layered-medium regularization ($\alpha = 0.999$) requires Full-Waveform IMPACT to change the depth placement of the image target. However, the objective function (3) is inherently resistant to those depth changes because of a cycle-skipping effect. In other words, if the gradient image primarily requires image targets to change their depth, the linearized change in the residuals $R_m(\vec{x}_k^{im}; \vec{s})$ becomes large, resulting in an overly conservative (or small) step size during the conjugate gradient algorithm. The formula in (11) was designed to counteract this effect.

This resistance to depth changes in the imaging target ultimately points back to the overarching issue of cycle-skipping as the source of non-convexity in (3). However, it is not the cycle skipping between images $I_m(\vec{x}_k^{im}; \vec{s})$ and $I_{m+1}(\vec{x}_k^{im}; \vec{s})$ that is problematic: aberrations between $I_m(\vec{x}_k^{im}; \vec{s})$ and $I_{m+1}(\vec{x}_k^{im}; \vec{s})$ are often much smaller than a half cycle. Instead, imaging targets are themselves cycle-skipped relative to their true positions in the image. Therefore, the velocity-depth ambiguity is linked to the problem of cycle skipping in pulse-echo ultrasound, which ultimately explains the false local minima in the estimation-correction problem.

There may be ways to overcome these false local minima during Full-Waveform IMPACT. In seismic imaging literature, one strategy to overcome cycle skipping is adaptive waveform inversion [16]. Additionally, there are several alternative objective functions for WEMVA [13] that could be utilized for the inversion. Recent work uses an automatic differentiation software called JAX to solve the estimation-correction problem [17]. While JAX offers the most generality when evaluating a variety of difficult-to-differentiate objective functions, the memory cost of retaining the full image reconstruction pipeline may become too large. In these cases, it would be better to rely on adjoint-state methods with much a simpler objective function such as the one presented here.

IV. Conclusions and Future Work

We demonstrate a ray-based alternative to WEMVA that we label as Full-Waveform IMPACT. In each of two k-Wave simulations, Full-Waveform IMPACT shows that the choice of regularization impacts the estimated sound speed and aberration correction by virtue of the non-convexity of the problem. This non-convexity of this problem comes in the form of cycle skipping, which appears to play a role in the velocity-depth ambiguity. By linking the velocity-depth ambiguity to cycle skipping, our future work will be motivated by solutions to the cycle-skipping problem that simultaneously address the velocity-depth ambiguity.

Acknowledgment

We would like to acknowledge the sound speed imaging group at Stanford University (Thurston Brevett, Sergio Sanabria, Tony Podkowa, Hanna Bendjador, Scott Hsieh, Walter Simson, Louise Zhuang, and Dongwoon Hyun) for valuable scientific discussions that motivated this work. This work was funded by University of Rochester Medical Center and the National Institute of Biomedical Imaging and Bioengineering (NIBIB) under grant F32-EB034589.

References

[1] J. J. Dahl, S. A. McAleavey, G. F. Pinton, M. S. Soo, and G. E. Trahey, "Adaptive imaging on a diagnostic ultrasound scanner at quasi real-time rates," *IEEE transactions on ultrasonics, ferroelectrics, and frequency control*, vol. 53, no. 10, pp. 1832–1843, 2006.

[2] J. C. Tillett, J. P. Astheimer, and R. C. Waag, "A model of distributed phase aberration for deblurring phase estimated from scattering," *IEEE transactions on ultrasonics, ferroelectrics, and frequency control*, vol. 57, no. 1, pp. 214–228, 2009.

[3] M. Fink, "Time reversal of ultrasonic fields. i. basic principles," *IEEE transactions on ultrasonics, ferroelectrics, and frequency control*, vol. 39, no. 5, pp. 555–566, 1992.

[4] M. Jaeger, G. Held, S. Peeters, S. Preisser, M. Grünig, and M. Frenz, "Computed ultrasound tomography in echo mode for imaging speed of sound using pulse-echo sonography: proof of principle," *Ultrasound in medicine & biology*, vol. 41, no. 1, pp. 235–250, 2015.

[5] R. Rau, D. Schweizer, V. Vishnevskiy, and O. Goksel, "Speed-of-sound imaging using diverging waves," *International Journal of Computer Assisted Radiology and Surgery*, vol. 16, no. 7, pp. 1201–1211, 2021.

[6] P. Stähli, M. Kuriakose, M. Frenz, and M. Jaeger, "Improved forward model for quantitative pulse-echo speed-of-sound imaging," *Ultrasonics*, vol. 108, p. 106168, 2020.

[7] R. Rau, D. Schweizer, V. Vishnevskiy, and O. Goksel, "Ultrasound aberration correction based on local speed-of-sound map estimation," in *2019 IEEE International Ultrasonics Symposium (IUS)*. IEEE, 2019, pp. 2003–2006.

[8] R. Ali, T. Brevett, D. Hyun, L. L. Brickson, and J. J. Dahl, "Distributed aberration correction techniques based on tomographic sound speed estimates," *IEEE Transactions on Ultrasonics, Ferroelectrics, and Frequency Control*, vol. 69, no. 5, pp. 1714–1726, 2022.

[9] A. S. Podkowa and M. L. Oelze, "The convolutional interpretation of registration-based plane wave steered pulse-echo local sound speed estimators," *Physics in Medicine & Biology*, vol. 65, no. 2, p. 025003, 2020.

[10] S. H. Bickel, "Velocity-depth ambiguity of reflection traveltimes," *Geophysics*, vol. 55, no. 3, pp. 266–276, 1990.

[11] R. Ali, T. M. Mitcham, M. Singh, M. M. Doyley, R. R. Bouchard, J. J. Dahl, and N. Duric, "Sound speed estimation for distributed aberration correction in laterally varying media," *IEEE Transactions on Computational Imaging*, vol. 9, pp. 367–382, 2023.

[12] R. Ali, T. Mitcham, M. Singh, R. Bouchard, J. Dahl, M. Doyley, and N. Duric, "Distributed aberration correction in handheld ultrasound based on tomographic estimates of the speed of sound," in *Medical Imaging 2023: Ultrasonic Imaging and Tomography*, vol. 12470. SPIE, 2023, pp. 25–35.

[13] F. Perrone, P. Sava, C. Andreoletti, and N. Bienati, "Linearized wave-equation migration velocity analysis by image warping," *Geophysics*, vol. 79, no. 2, pp. S35–S46, 2014.

[14] R. Ali, "Open-source full-waveform ultrasound computed tomography based on the angular spectrum method using linear arrays," in *Medical Imaging 2022: Ultrasonic Imaging and Tomography*, vol. 12038. SPIE, 2022, pp. 187–205.

[15] B. E. Treeby and B. T. Cox, "k-wave: Matlab toolbox for the simulation and reconstruction of photoacoustic wave fields," *Journal of biomedical optics*, vol. 15, no. 2, p. 021314, 2010.

[16] M. Warner and L. Guasch, "Adaptive waveform inversion: Theory," *Geophysics*, vol. 81, no. 6, pp. R429–R445, 2016.

[17] W. Simson, L. Zhuang, S. J. Sanabria, N. Antil, J. J. Dahl, and D. Hyun, "Differentiable beamforming for ultrasound autofocusing," in *International Conference on Medical Image Computing and Computer-Assisted Intervention*. Springer, 2023.